Journal of The Electrochemical Society

The Electrochemical Society
Advancing solid state & electrochemical science & technology

Relationship between Copper(II)-Lactate Complexes and Cu_2O Electrodeposited Using Highly Concentrated Alkaline Solutions

To cite this article: Ryutaro Miura *et al* 2023 *J. Electrochem. Soc.* **170** 092508

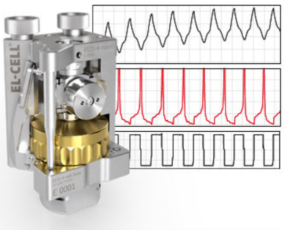

Journal of The Electrochemical Society, 2023 **170** 092508

Relationship between Copper(II)-Lactate Complexes and Cu_2O Electrodeposited Using Highly Concentrated Alkaline Solutions

Ryutaro Miura,[1] Ryusuke Yuasa,[1] Tsutomu Shinagawa,[2] Kazuhiro Fukami,[1,*] and Kuniaki Murase[1,*,z]

[1]Department of Materials Science and Engineering, Kyoto University, 36-1 Yoshida-hommachi, Sakyo-ku, Kyoto 606-8501, Japan
[2]Research Division of Electronic Materials, Morinomiya Center, Osaka Research Institute of Industrial Science and Technology, Osaka 536-8553, Japan

The direct or indirect effects of two different copper(II)-lactate complex species, $Cu(H_{-1}L)L^-$ and $Cu(H_{-1}L)_2{}^{2-}$, on the orientation and electrical properties of Cu_2O electrodeposits were examined, where $L^- = CH_3CH(OH)COO^-$ and $H_{-1}L^{2-} = CH_3CH(O^-)COO^-$. To investigate the relationships between the copper(II)-lactate complex species and several properties of Cu_2O, a set of Cu_2O layers was electrodeposited from thermodynamically well-stabilized electrolytes of different pHs with unified overpotentials. The Cu_2O layers obtained at pH <9.5 had the ⟨100⟩ preferential orientation, whereas the orientation changed to the ⟨111⟩ preferential orientation at pH >9.5. In addition, marked differences were observed in the resistivity and carrier density of Cu_2O layers bordering pH 9.5, indicating the presence of a strong relationship between copper(II)-lactate complexes and these crystallographic or electrical properties. In terms of the cathodic reactivity of copper(II)-lactate complexes and changes in local pH in the vicinity of the cathode upon electrodeposition, we suggest that the two copper(II)-lactate complexes directly affected the electrical properties of Cu_2O and indirectly affected its crystallographic orientation.

[DOI: 10.1149/1945-7111/acf792]

Manuscript submitted July 19, 2023; revised manuscript received August 29, 2023. Published September 26, 2023.

Cuprous oxide (Cu_2O), or copper(I) oxide, is a p-type semiconductor with a direct band gap of approximately 2 eV,[1,2] which has potential as a material for solar cells, photoelectrodes, and photocatalysts due to its low cost and toxicity. The electrodeposition method using aqueous electrolytes has the following advantages over conventional vapor deposition processes, such as magnetron sputtering[3] and molecular beam epitaxial growth:[4] low cost, low environmental impact, and high controllability. Many studies have examined Cu_2O electrodeposition from aqueous alkaline electrolytes, in which α-hydroxycarboxylates, such as citrate[5] and tartarate,[6] are added as complexing ligands, with lactate being the most common complexing ligand.[7–10]

The photoelectric performance of Cu_2O is affected by its crystallographic microstructure. The resistivity of Cu_2O layers varies with their orientation. Cu_2O with the ⟨111⟩ orientation, which may contain many intrinsic point defects, has been reported to have the lowest resistivity.[11] Furthermore, Cu_2O with {111} facets has the highest photocatalytic activity.[12] In the case of Cu_2O/ZnO solar cells, the basal plane of ZnO has a minimized misfit with the {111} plane of Cu_2O.[13] Therefore, it is important to control the preferred orientation and concomitant surface morphology of electrodeposited Cu_2O for its application to specific devices.

Previous studies demonstrated that the orientation of electrodeposited Cu_2O was dependent on the pH and current density of electrolytes.[7–9,14–16] Cu_2O with the ⟨100⟩ orientation was obtained from electrolytes of pH 9.0–9.5, and that with the ⟨111⟩ orientation from electrolytes of pH 12.0–12.5.[7–9,14,15] Furthermore, even if an electrolyte of the same pH is used, the orientation of Cu_2O depends on current density; Cu_2O with the ⟨100⟩ orientation was obtained below 1.4 mA cm^{-2} and that with the ⟨111⟩ orientation above 2.0 mA cm^{-2} in an electrolyte of pH 9.0.[16] In addition to its orientation, the crystal morphology of Cu_2O may be controlled by the electrolyte pH, electrodeposition potential, and current density.[16,17]

The thermodynamic and kinetic behaviors of electrodeposition and some of the properties of the resulting electrodeposits, including their crystallographic morphology, are dependent on the state of the species being reduced by the electrochemical reaction. In the case of Cu_2O electrodeposition, it is natural to assume that the crystallographic orientation of the Cu_2O layer is affected by copper(II) complexes in the electrolyte. In previous studies,[7–9,14–17] Cu_2O electrodeposition was performed without identifying the copper(II)-lactate complex species in alkaline copper(II)-lactate electrolytes. Therefore, an investigation of the relationships between copper(II)-lactate complex species and the properties of electrodeposited Cu_2O from copper(II)-lactate electrolytes has not been possible.

Our research group recently identified two different copper(II)-lactate complexes that formed in the alkaline region in a pH-dependent manner.[18] We calculated their stability constants, which made it possible to draw a potential-pH diagram of the Cu-lactate-H_2O system.[19] Therefore, the groundwork is now laid for a detailed study on the relationships among copper(II)-lactate complex species, the behavior of their Cu_2O electrodeposits, and the properties of the Cu_2O obtained. In Fig. 1, newly drawn potential-pH and pH-speciation diagrams of the Cu-lactate-H_2O system, in which two new copper(II)-lactate complexes, $Cu(H_{-1}L)L^-$ and $Cu(H_{-1}L)_2{}^{2-}$, are stable at pH > 7,[18,19] show the equilibrium potential between each complex and Cu_2O. Since there are no data on the equilibrium potentials of Cu_2O electrodeposition in the alkaline region, a discussion on the exact overpotential, or driving force, of Cu_2O deposition has been impossible to date. For example, to examine the pH dependence of Cu_2O electrodeposition behavior, a comparison of this behavior with a unified overpotential is required in order to reduce the number of parameters that need to be considered; however, this has not been possible. A previous study demonstrated that the orientation of Cu_2O and semiconductor properties, such as the resistivity of Cu_2O, depended on the electrodeposition potential;[9] however, the extent to which the electrodeposition potential corresponded to an overpotential from the equilibrium potential was not discussed. The identification of copper(II)-lactate complexes has made these discussions possible.

We obtained another important finding on the two copper(II)-lactate complexes in the alkaline region: the change over time in the visible absorption spectrum of the electrolyte after its preparation indicated that these complexes require at least 24 h to equilibrate.[18] Therefore, aging of the electrolyte for at least 24 h is necessary to perform electrodeposition experiments with good reproducibility.

---

*Electrochemical Society Member.
zE-mail: murase.kuniaki.2n@kyoto-u.ac.jp

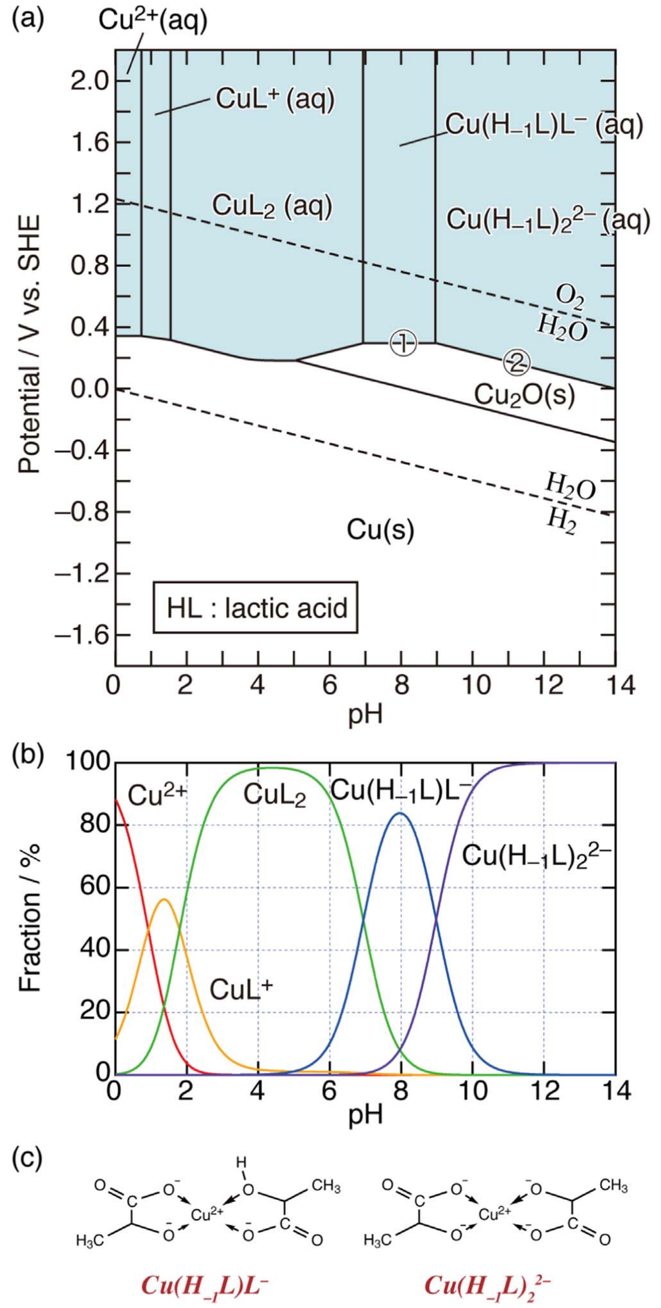

Figure 1. (a) A potential-pH diagram (298 K) of the Cu-lactic acid(HL)-H_2O system, and (b) a pH-speciation diagram, based on our previous study.[19] In both diagrams, the analytical concentrations of Cu(II) and lactic acid were 0.4 and 3.0 M, respectively. Note that the unit of the potential axis of (a) is V vs SHE (standard hydrogen electrode); the value is +0.206 V larger than V vs Ag/AgCl in 3.33 M KCl. (c) Structures of $Cu(H_{-1}L)L^-$ and $Cu(H_{-1}L)_2^{2-}$, where $H_{-1}L^{2-}$ is a deprotonated lactate ion.

However, there is no indication that previous studies[7–9,14–17] on Cu_2O electrodeposition considered the adequate aging of the electrolyte.

In the present study, we prepared a set of thermodynamically well-stabilized copper(II)-lactate alkaline electrolytes and electrodeposited Cu_2O under conditions of different pH, but a unified overpotential from the thermodynamic equilibrium potential at each pH. The effects of the pH-dependent copper(II)-lactate complex species (Fig. 1b) on the orientation and electrical properties of Cu_2O electrodeposits were then examined.

Experimental

All electrolytes were prepared with reagent-grade chemicals purchased from Nacalai Tesque and deionized water (resistivity of 18 MΩ cm) obtained using a Milli-Q system. Copper(II)-lactate electrolytes with different pH for Cu_2O electrodeposition contained 0.4 M (M = mol dm^{-3}) copper(II) acetate monohydrate ($Cu(CH_3COO)_2{\cdot}H_2O$) and 3.0 M lactic acid ($CH_3CH(OH)COOH$). Since commercially available lactic acid contains approximately 10% water, electrolytes were prepared accordingly. The pH of electrolytes was adjusted using NaOH. Prior to Cu_2O electrodeposition, the electrolyte was aged for 1 day to complete complexation processes.[18] Electrodeposition was performed using a potentiostat (SP-50, Bio-Logic Science Instruments) and a three-electrode cell with a conductive fluorine-doped crystalline tin oxide (FTO)-coated glass as the working electrode, a Pt sheet as the counter electrode, and Ag/AgCl in 3.33 M KCl as the reference electrode. Electrodeposition potentials were set at a cathodic overpotential of 0.3, 0.4, 0.5, or 0.6 V relative to the equilibrium potential of the $Cu(H_{-1}L)^-/Cu_2O$ or $Cu(H_{-1}L)_2^{2-}/Cu_2O$ redox pair indicated by line ① or ② in Fig. 1a. According to thermochemical data,[19] the equilibrium potentials E_{eq} of lines ① ($6.95 < pH < 8.95$) and ② ($pH > 8.95$) are given by

$$E_{eq} = +0.085[\text{V vs Ag/AgCl}] \qquad [1]$$

and

$$E_{eq} = +0.618 - 0.0591\text{pH}[\text{V vs Ag/AgCl}] \qquad [2]$$

for electrolytes containing 0.4 M Cu(II) and 3.0 M lactic acid as the analytical concentrations. Therefore, when electrodepositing at a cathodic overpotential of 0.5 V using an electrolyte of pH 8.2, the potential was set to –0.415 V vs Ag/AgCl; for electrodeposition at a cathodic overvoltage of 0.3 V using an electrolyte of pH 11.5, the cathodic potential was set to –0.361 V vs Ag/AgCl. The total electric charge for each electrodeposition run was basically unified to 2.0 C cm^{-2}. In resistivity (or specific resistance) measurements using the van der Pauw method, thicker Cu_2O electrodeposits (5.0 C cm^{-2}) were also prepared to reduce the electrical resistance of films. These electric charges corresponded to approximately 2.5 and 6.1 μm of the thickness of Cu_2O when electrodeposition efficiency was 100%.

The resulting electrodeposits were characterized using a field-emission scanning electron microscope (FE-SEM; JEOL JSM-6500F) and X-ray diffractometer (XRD; Rigaku RINT-2200) with Cu-Kα radiation at 40 kV and 30 mA. The resistivity and Hall effect (carrier density) of electrodeposits were evaluated with RsiTest8310 (Toyo Corp.) using the van der Pauw method at room temperature. A set of squared Cu_2O samples for resistivity and Hall effect measurements were prepared using the method of Miyake et al.[20] to remove electrodeposits from the conductive substrate and transfer them onto non-conductive epoxy resin (Araldite; HUNTSMAN). Silver paste was attached to the four corners of the squared sample as metal electrodes to connect to the measurement apparatus.

Results and Discussion

Structural characterization of Cu_2O electrodeposits.—Figure 2 summarizes the XRD patterns of Cu_2O layers on the FTO substrate electrodeposited at an overpotential of 0.3, 0.4, 0.5, or 0.6 V using electrolytes with pH 8.2, 9.4, 9.9, 10.3, or 11.5. In all electrodeposits, diffraction peaks corresponding to cubic Cu_2O were observed at $2\theta = 29.6°$ (110), 36.4° (111), 42.3° (200), and 62.3° (220).

The orientation of Cu_2O electrodeposits with respect to the flat FTO substrate was evaluated using the following Willson equation.[21,22]

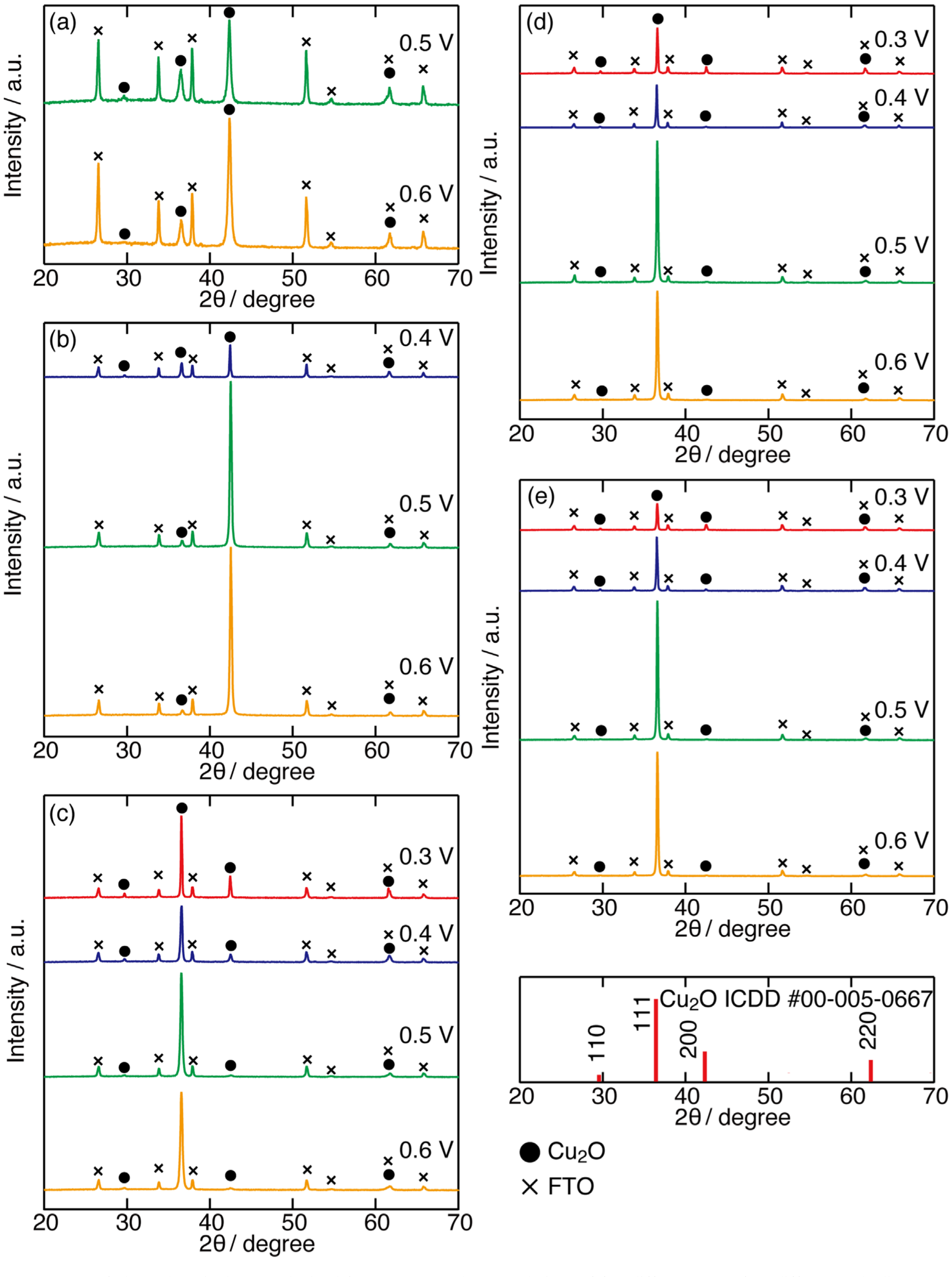

Figure 2. XRD patterns of electrodeposited Cu_2O obtained from copper(II)-lactate solutions of five different pH at four different cathodic overpotentials in a range 0.3–0.6 V: (a) pH 8.2, (b) pH 9.4, (c) pH 9.9, (d) pH 10.3, and (e) pH 11.5. No deposits were obtained with an overpotential of 0.3–0.4 V and 0.3 V at pH 8.2 and pH 9.4, respectively.

$$\text{Orientation index}(N) = \frac{\left(\dfrac{\mathrm{I}_{hkl}}{\sum \mathrm{I}_{hkl}}\right)}{\left(\dfrac{\mathrm{I}_{0,hkl}}{\sum \mathrm{I}_{0,hkl}}\right)} \qquad [3]$$

where I_{hkl} is the relative intensity of the diffraction peak corresponding to each *hkl* reflection, $I_{0,hkl}$ is the relative intensity of the *hkl* reflection of a powder diffraction file (ICDD ♯00–005–0667), and ΣI_{hkl} and $\Sigma I_{0,hkl}$ are the sum of the diffraction intensity ratios for all three indices, i.e., $hkl = 111, 200, 220$. An orientation index (N) for a given diffraction that approached 1 indicated that the direction corresponding to that diffraction was not preferentially oriented. Figure 3 summarizes the orientation indices (N) calculated by Eq. 3 based on the XRD patterns in Fig. 2. Electrodeposited Cu_2O basically has the ⟨100⟩ orientation at pH 8.2 and pH 9.4 and the ⟨111⟩ orientation at pH 9.9 or higher, regardless of the overpotential. It is important to note that orientation significantly changes across the narrow region between pH 9.4 and pH 9.9. At pH >9.9, the orientation indices of 111 and 200 diffraction are closer to 1 at an overpotential of 0.3 V than at an overpotential of 0.4 V or higher, suggesting that the overpotential also affects the orientation. However, no significant change from the ⟨100⟩ to ⟨111⟩ preferential orientation simply by increasing the cathodic overpotential was recognized, as reported in previous studies.[23,24] The reason for this remains unclear, but may be because previous studies did not focus on achieving the equilibrium of complex formation when preparing electrolytes, as in the present study. Nevertheless, the contribution of the overpotential to the orientation was small. The pH speciation diagram of the copper(II)-lactate electrolyte in Fig. 1b indicates that the pH region at which the fraction of $Cu(H_{-1}L)_2{}^{2-}$ was dominant coincided well with the region at which Cu_2O with the ⟨111⟩ preferential orientation was electrodeposited. As pH decreased, the fraction of $Cu(H_{-1}L)L^{-}$ increased and the orientation changed to ⟨100⟩, indicating a level of synchrony. The orientation indices of the 111 diffraction of Cu_2O obtained from the three electrolytes at pH 9.9, 10.3, and 11.5 with the same overpotential were similar. In this pH range, the fraction of $Cu(H_{-1}L)_2{}^{2-}$ was >90%. These results strongly suggest that pH-dependent differences in copper(II)-lactate complex species correlated with the orientation of the resulting Cu_2O.

Figure 4 shows surface FE-SEM images of Cu_2O electrodeposited from electrolytes at pH 8.2, 9.4, 9.9, 10.3, and 11.5 with a cathodic overpotential of 0.5 V. At pH 9.9 or higher, the surface of Cu_2O deposits was composed of triangular pyramidal grains with vertexes pointing perpendicular to the substrate, whereas at lower pH, square pyramidal grains were observed. In consideration of the results obtained on the preferential orientation by XRD, the side faces of each triangular pyramidal crystal grain corresponded to the three {100} facets of the cubic crystal, and the direction perpendicular to the base of the pyramidal crystals was the ⟨111⟩ direction. Similarly, the side faces of each square pyramidal crystal grain corresponded to the four {111} facets, and the direction from the base to the vertexes perpendicularly was the ⟨100⟩ direction.

Electrical properties of Cu_2O electrodeposits.—Figure 5a shows the resistivity of Cu_2O electrodeposited at a cathodic overpotential of 0.5 V with electric charges 5.0 C cm^{-2} from the electrolytes at pH 8.3, 9.3, 9.8, 10.0, and 11.3. Multiple plots at the same pH are shown in Fig. 5a because multiple samples were prepared at the same pH and assessed to verify measurement variability and experimental reproducibility. The resistivity of electrodeposited Cu_2O obtained at pH 9.3 or lower was generally in the order of 10^7 Ω cm or higher; resistivity gradually decreased with increasing pH. In contrast, the resistivity of electrodeposited Cu_2O obtained at pH 9.8 or higher was approximately 1×10^6 Ω cm lower and almost constant irrespective of pH. Figure 1b shows that the fraction of complex species was dependent on pH up to approximately pH 9.5; however, at pH >9.5, the fraction of $Cu(H_{-1}L)_2{}^{2-}$ became almost constant towards 100%. This result indicated that copper(II)-lactate complex species also affect the resistivity of electrodeposited Cu_2O. The manner in which copper(II)-lactate species are causally related to the resistivity and the orientation of resulting Cu_2O is discussed below.

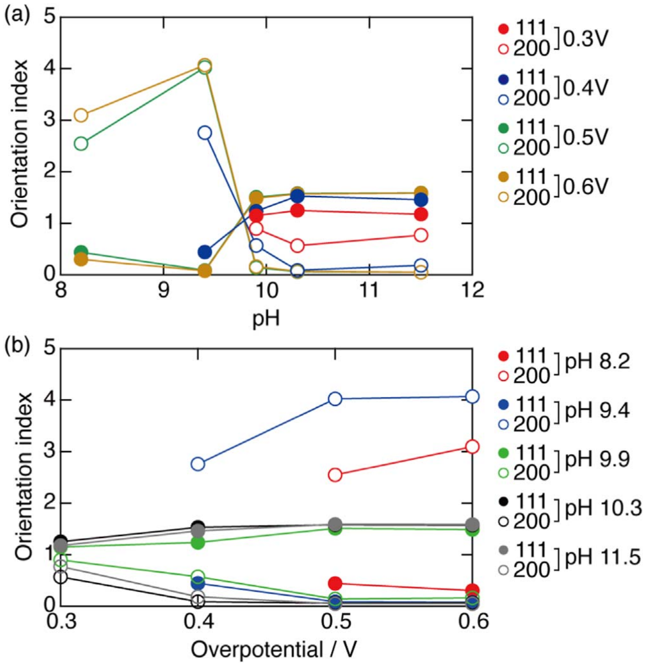

Figure 3. Orientation indices of electrodeposited Cu_2O obtained from five different pH copper(II)-lactate solutions with a cathodic overpotential ranging from 0.3 to 0.6 V: (a) pH dependence and (b) cathodic overpotential dependence.

Figure 5b shows the carrier density of the same Cu_2O samples. The carrier densities of Cu_2O electrodeposited at pH 9.8 or higher were in the order of 10^{12} cm^{-3} with good reproducibility, whereas those from pH 9.3 and 8.3 were 10^{10}–10^{11} cm^{-3}, with poor reproducibility. The reason for this result may be that the carrier density of Cu_2O electrodeposits obtained from a low pH was very small and close to the measurement limit of the instrument used. Copper(II)-lactate complex species are considered to affect the carrier density.

Figure 5c summarizes the average deposition current densities during each Cu_2O electrodeposition to prepare samples for Hall effect measurements. The current density showed a large difference by a factor of 10 between pH 9.3 and pH 9.8. This was similar to the results obtained on orientation and resistivity, suggesting the direct or indirect effects of copper(II)-lactate complex species. The low current density at low pH appeared to be due to Cu_2O electrodeposits with high resistivity. As electrodeposition progresses, carrier transport within the resulting Cu_2O is considered to become the rate-limiting factor for electrodeposition.

The relationship between copper(II)-lactate complexes and electrical properties of the resulting Cu_2O.—The present results indicate that relationships exist between copper(II)-lactate complex species and orientation, resistivity, or carrier density. In this section, we discuss a potential mechanism by which copper(II)-lactate complex species affect the electrical properties.

Cu_2O generally exhibits p-type semiconductor properties with intrinsic Cu defects.[25,26] Therefore, the conductivity of Cu_2O depends on the amount of Cu defects introduced and the origin of p-type carriers. The Cu_2O electrodeposition reaction is considered to take place via the intermediate, $Cu^{I}OH$.[16,27] If that is the case, the

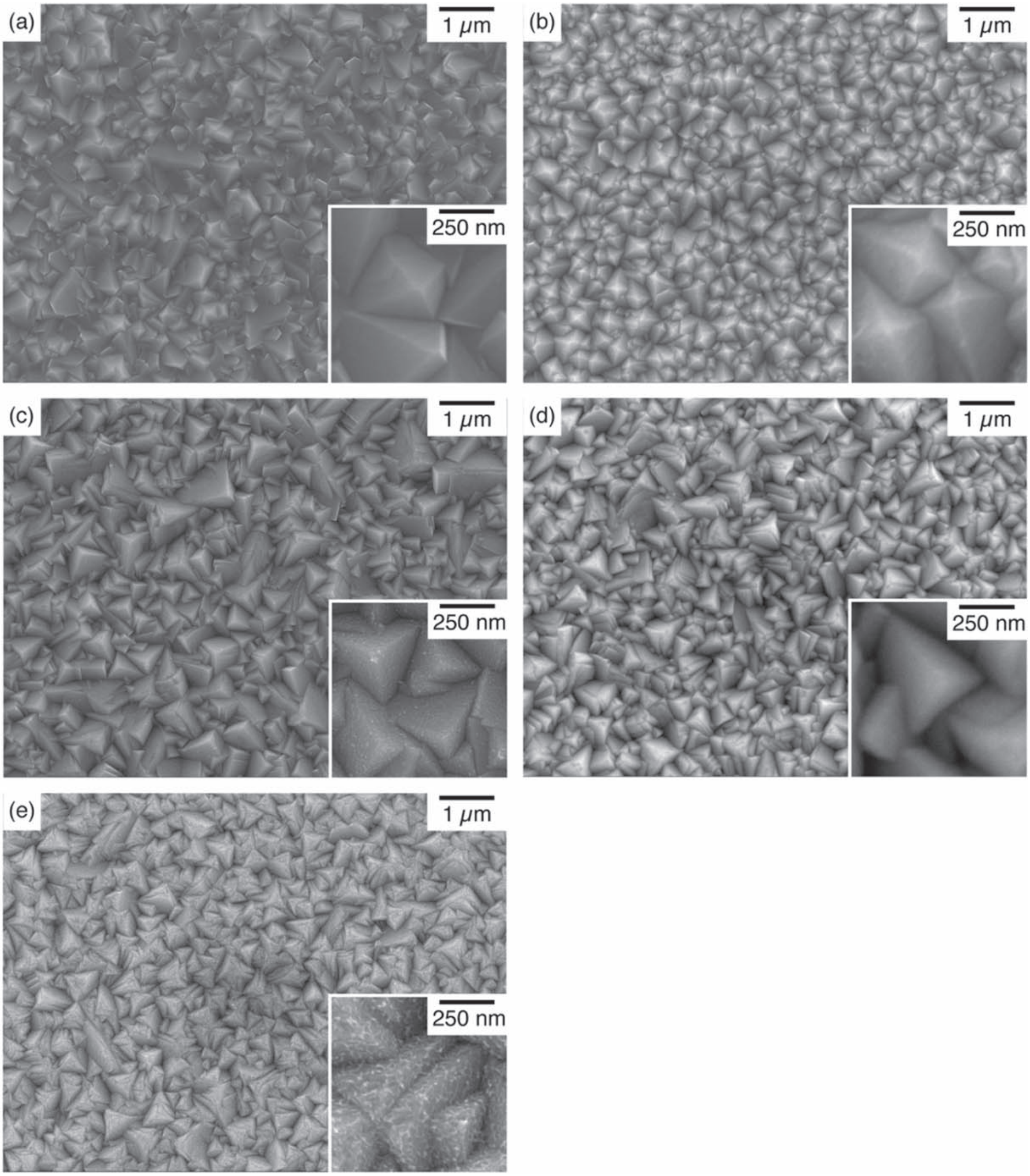

Figure 4. FE-SEM surface images of electrodeposited Cu_2O obtained from five different pH copper(II)-lactate solutions at a cathodic overpotential of 0.5 V: (a) pH 8.2, (b) pH 9.4, (c) pH 9.9, (d) pH 10.3, and (e) pH 11.5.

deposition reaction is represented by the reduction of copper(II)-lactate complexes to form Cu^IOH accompanying desolvation:

$$Cu(H_{-1}L)L^- + H_2O + e = Cu^IOH + 2L^- \quad \text{(at low pH)} \qquad [4]$$

$$Cu(H_{-1}L)_2{}^{2-} + 2H_2O + e = Cu^IOH + 2L^- + OH^- \ \text{(at high pH)} \qquad [4']$$

followed by the decomposition of Cu^IOH to form Cu_2O:

$$2Cu^IOH = Cu_2O + H_2O \qquad [5]$$

As long as these reactions occur according to stoichiometry, no defects in Cu^+ ions are expected. However, defects in Cu^+ ions often occur in Cu_2O crystals because O^{2-} ions are incorporated into the crystal lattice independently of the decomposition of Cu^IOH, for example, by:

$$OH^- = O^{2-} + H^+ \qquad [6]$$

Therefore, the amount of Cu^+ defects may be affected by how quickly the reduction of copper(II)-lactate complexes occurs. We considered the lower carrier density and concomitant higher resistivity of Cu_2O deposited from lower pH electrolytes to be due to the faster reduction of copper(II)-lactate complexes in this electrolyte. The rate of an electrode reaction is generally governed by kinetic and thermodynamic factors unless the reaction is controlled by mass transfer of reactant(s) from the bulk electrolyte to the electrode surface. Considering the low average current density (<1 mA cm^{-2}; Fig. 5c) and the high concentration of Cu(II) species

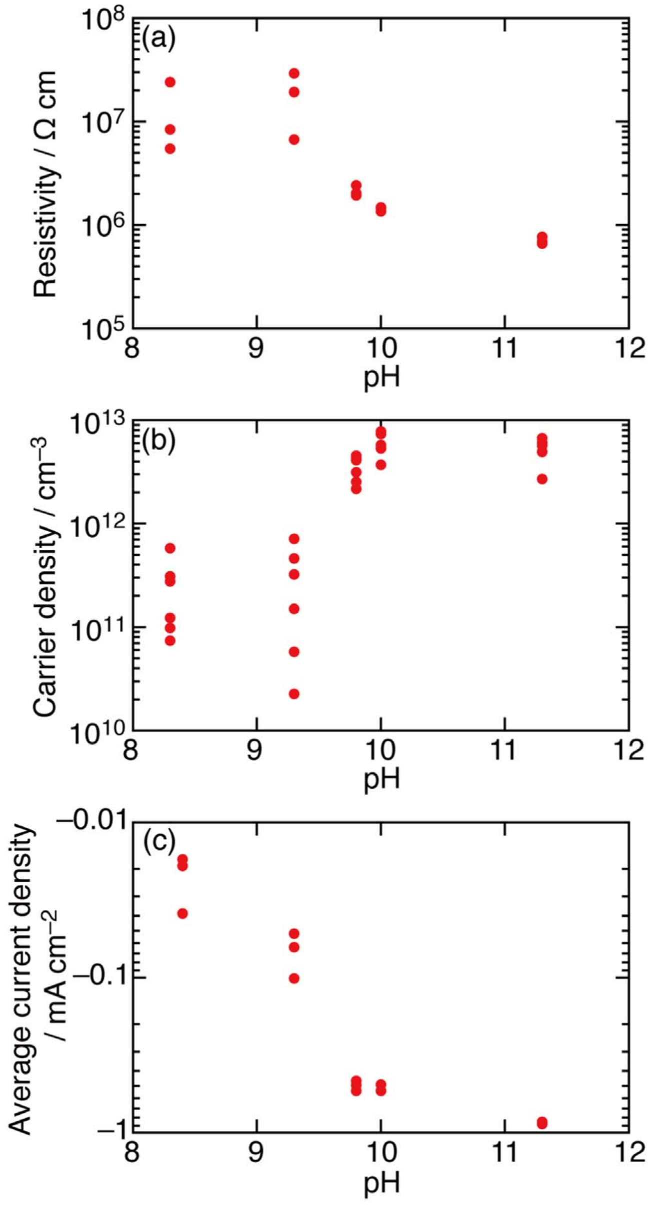

Figure 5. (a) Resistivity and (b) carrier density of electrodeposited Cu_2O, and (c) average current density during Cu_2O electrodeposition. Electrodeposition was performed at a cathodic overpotential of 0.5 V from copper(II)-lactate solutions at pH 8.3, 9.3, 9.8, 10.0, and 11.3.

(0.4 M), it is obvious that the Cu_2O deposition in this study is not controlled by the mass transfer of Cu(II) species. In addition, since the present study compared electrodeposition behaviors by unifying the overpotential (i.e., 0.5 V) or thermodynamic driving force, the dominant factor was considered to be limited to kinetic factors. In other words, the copper(II)-lactate complex in the low pH region, $Cu(H_{-1}L)L^-$, was considered to be kinetically reduced more easily than the other complex that was dominant in the high pH region, $Cu(H_{-1}L)_2{}^{2-}$ (see Fig. 1b).

In the electrodeposition process, complexes with lower symmetry are more favorable to react than those with higher symmetry, both in terms of thermodynamics and kinetics, resulting in straightforward electrodeposition.[28–30] For example, in the case of aluminum (Al) electrodeposition from chloroaluminate ionic liquids in which $Al_2Cl_7{}^-$ and $AlCl_4{}^-$ species coexist in the electrolyte, $Al_2Cl_7{}^-$ with lower symmetry is known to be preferentially reduced to the electrodeposit metallic Al.[28] In the case of the aqueous electrodeposition of a Ni-Mo alloy in which the reduction of molybdenum species is induced by nickel deposition, the less symmetrical 1:1 complex of the Ni(II)-citrate system, $Ni(Cit)^-$, was shown to be more easily reduced than the symmetrical 1:2 complex, $Ni(Cit)_2{}^{4-}$ ($Cit^{3-} = C_6H_5O_7{}^{3-}$), resulting in the better performance of induced co-deposition.[30] In comparisons of the $Cu(H_{-1}L)L^-$ complex with $Cu(H_{-1}L)_2{}^{2-}$, it is clear from the potential-pH diagram that the former complex was more thermodynamically reducible because the equilibrium potential of the $Cu(H_{-1}L)L^-/Cu_2O$ pair (Eq. 1) was more positive than that of the $Cu(H_{-1}L)_2{}^{2-}/Cu_2O$ pair (Eq. 2). Furthermore, $Cu(H_{-1}L)L^-$ with lower symmetry was kinetically reduced more easily than $Cu(H_{-1}L)_2{}^{2-}$. When electrodeposited at higher cathodic overpotentials, electrolytes dominated by $Cu(H_{-1}L)L^-$ often gave the co-deposition of metallic Cu, whereas those dominated by $Cu(H_{-1}L)_2{}^{2-}$ did not (data not shown), which indicated that $Cu(H_{-1}L)L^-$ was more readily reduced than $Cu(H_{-1}L)_2{}^{2-}$.

The formation of Cu^+ defects may also be attributed to the concentration of OH^- in the vicinity of the cathode in addition to a difference in the copper(II)-lactate complex. At lower pH, the independent incorporation of O^{2-} through, for example, reaction 6 is restricted due to the low activity of OH^-. In contrast, electrolytes of high pH exhibiting higher OH^- activities provide an environment conducive to Cu^+ defects. Moreover, the overall reaction of Cu_2O electrodeposition from $Cu(H_{-1}L)_2{}^{2-}$ complexes in electrolytes of high pH, given by the sum of reactions 4′ and 5:

$$2Cu(H_{-1}L)_2{}^{2-} + 3H_2O + 2e = Cu_2O + 4L^- + 2OH^- \qquad [7]$$

releases additional OH^- ions near the cathode, providing a higher pH environment and more Cu^+ defects. On the other hand, the overall deposition of Cu_2O from $Cu(H_{-1}L)L^-$ at a lower pH is

$$2Cu(H_{-1}L)L^- + H_2O + 2e = Cu_2O + 4L^- \qquad [8]$$

that does not change the activity of OH^- near the cathode, maintaining a low pH environment. As a result, a Cu_2O layer with few Cu^+ defects, low carrier density, and high resistivity may continuously be deposited from electrolytes containing $Cu(H_{-1}L)L^-$ as the dominant species. Due to the low carrier density of the resulting Cu_2O layer, deposition becomes limited by carrier diffusion, in spite of the high reactivity of $Cu(H_{-1}L)L^-$ complexes, showing a low deposition current density.

The relationship between copper(II)-lactate complexes, current density, and the orientation of Cu_2O.—The initial electrodeposition state of Cu_2O was investigated to discuss the mechanism underlying the orientation of Cu_2O. Figure 6 shows FE-SEM images of Cu_2O surfaces electrodeposited with lower electric charges of 0.1 and 0.5 C cm^{-2} from electrolytes at pH 9.1 and pH 12.6. Note that these electrolytes gave the ⟨100⟩ and ⟨111⟩ preferential orientations, respectively, when electrodeposited up to 2.0 C cm^{-2} or higher. The series of electrodeposition was performed at an overpotential of 0.5 V. Cu_2O was electrodeposited on glassy carbon instead of a crystalline FTO substrate to eliminate the possible effects of the substrate on the initial electrodeposition morphology through, for example, an epitaxy. However, another series of electrodeposition using a FTO substrate was performed for comparison, and no significant difference was observed in the initial morphology between the deposits on grassy carbon and those on FTO. At an electric charge of 0.1 C cm^{-2}, Cu_2O crystal grains with octahedral and cubic shapes were electrodeposited from electrolytes of pH 9.1 and 12.6, respectively, in a random orientation with no specific direction perpendicular to the substrate (Figs. 6a, 6b). In the electrodeposition of crystalline substances, the fastest crystal growth occurs in the direction perpendicular to the plane with the highest surface energy.[31] The highest energy plane then disappears, and the crystal becomes occupied by lower-energy planes. Regarding the cubic Cu_2O crystal, the {100} plane has a higher surface energy than

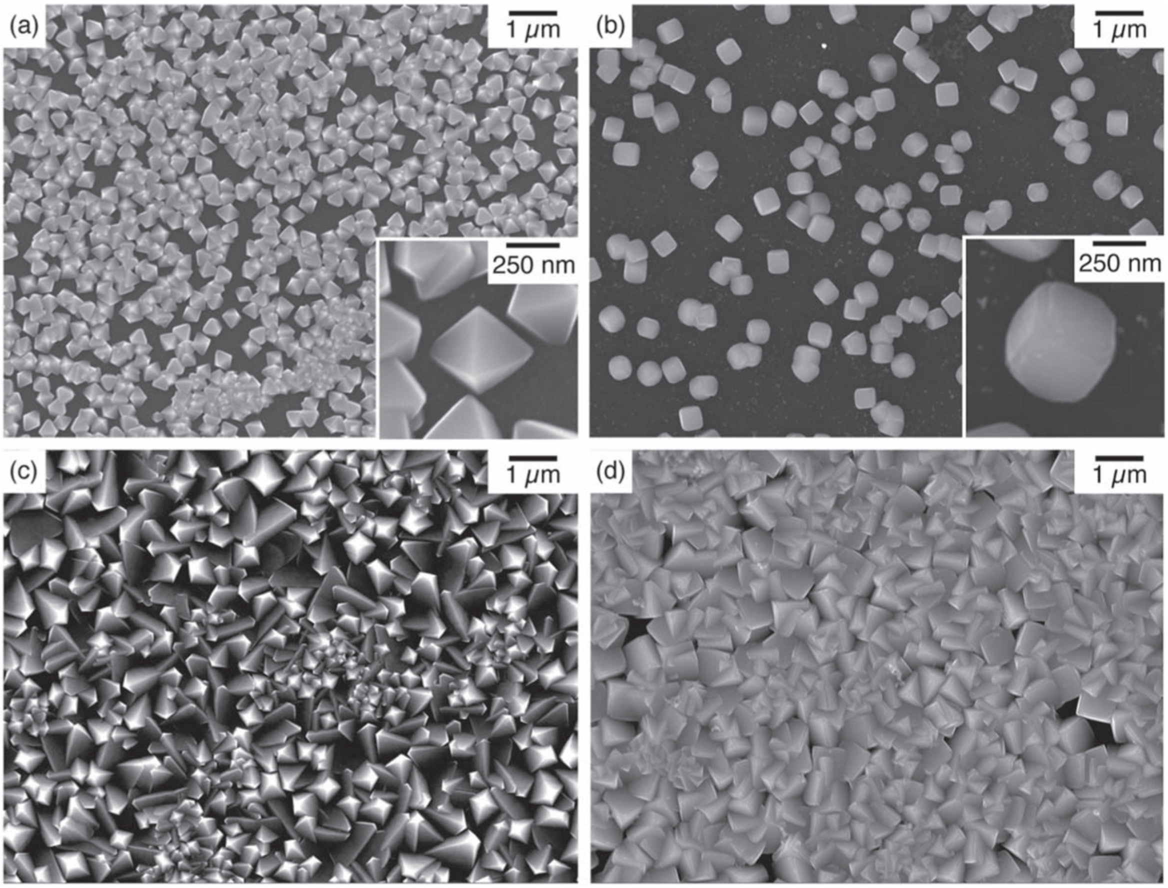

Figure 6. FE-SEM surface images of electrodeposited Cu_2O on glassy carbon from copper(II)-lactate solutions at (a), (c) pH 9.1 and (b), (d) pH 12.6: the electric charge was (a),(b) 0.1 C cm^{-2} and (c), (d) 0.5 C cm^{-2}.

the {111} plane, which is the most thermodynamically stable plane in Cu_2O.[32,33] Therefore, under low current density, namely, slow crystal growth with thermodynamic equilibrium control, the appearance of Cu_2O crystals with {111} facets is advantageous. In contrast, at high current densities, the condition favoring the appearance of {111} planes is weakened and crystals covered with {100} facets appear. Although the underlying mechanism remains unclear, the appearance of {100} facets, resulting in Cu_2O crystals with a cubic shape, may be related to the adsorption of lactate ions and/or OH^- ions (i.e., the formation of a Cu^IOH intermediate at the surface).

Regarding deposits at electric charges of 0.5 C cm^{-2} (Figs. 6c, 6d), the random orientation was lost and crystals with a vertex direction perpendicular to the substrate became predominant at pH 9.1 and pH 12.6. The external shape of the crystals of the cubic system is known to depend on the growth rate ratio, R, of the $\langle 100\rangle$ to $\langle 111\rangle$ directions.[34] R for octahedral- and cubic-shaped crystals are 1.73 and 0.58, respectively.[34] When these crystals were grown on a planar substrate, crystals with $R = 1.73$ and $R = 0.58$ grew the fastest in the $\langle 100\rangle$ and $\langle 111\rangle$ directions, respectively. Under this growth mode, crystals with a preferential growth direction that is not perpendicular to the substrate were eliminated as growth proceeded because these directions interfered with each other.

In summary, at low pH, current density was low due to Cu_2O with high resistivity, resulting in $\langle 100\rangle$-oriented Cu_2O with {111} facets, while at high pH, current density was high due to Cu_2O with low resistivity, resulting in $\langle 111\rangle$−oriented Cu_2O with {100} facets. Specifically, copper(II)-lactate complex species directly affected the carrier density and conductivity of electrodeposited Cu_2O and changes occur in current density depending on these electrical properties. Current density affects the crystal morphology of Cu_2O, and the orientation of Cu_2O is ultimately established during the crystal growth process. Therefore, an indirect correlation exists between pH–dependent copper(II)-lactate complexes and the crystallographic morphology of the resulting Cu_2O.

Conclusions

By taking advantage of our identification of two copper(II)-lactate complex species and their thermochemical constants in an alkaline region,[18,19] we investigated the relationships between copper(II)-lactate complexes and several properties of Cu_2O electrodeposits. Cu_2O electrodeposition was performed using copper(II)-lactate alkaline electrolytes under several different pH and a unified overpotential from the thermodynamic equilibrium potential at each pH, and correlations were observed between Cu_2O orientation, carrier density, and copper(II)-lactate complexes. Current density during Cu_2O electrodeposition under the unified overpotential showed a large difference between pH 9.3 and pH 9.8, suggesting that current depends on the resistivity of Cu_2O electrodeposits.

We discussed the relationship between copper(II)-lactate complexes and the properties of electrodeposited Cu_2O as follows: the carrier density and conductivity of electrodeposited Cu_2O are dependent on copper(II)-lactate complexes, while current density (i.e., the electrodeposition speed) is dependent on carrier density and conductivity. The electrodeposition speed affects the crystal morphology of Cu_2O. Crystals not growing perpendicularly to the substrate are eliminated through interference (collision) in the opposite directions, resulting in the formation of oriented electrodeposits. In summary, copper(II)-lactate complex species directly affect the carrier density and conductivity of electrodeposited Cu_2O and indirectly affect the crystal morphology and orientation of electrodeposited Cu_2O.

The present results show the relationship between complexes in aqueous electrolytes and electrodeposited semiconductors, and also demonstrate the importance of interpreting semiconductor electrodeposition based on thermodynamic data, such as the equilibrium constants of complexes.

Acknowledgments

We would like to thank Professor Atsushi Kitada (The University of Tokyo) for his collaboration with this work. This work was financially supported by a Grant-in-Aid for Scientific Research (S) (Grant No. 20H05663; K. M.) from the Japan Society for the Promotion of Science (JSPS) and a Grant-in-Aid for JSPS Fellows (Grant No. 22J15852; R. M.).

ORCID

Ryutaro Miura https://orcid.org/0009-0003-1679-8475
Tsutomu Shinagawa https://orcid.org/0000-0001-5671-1512
Kazuhiro Fukami https://orcid.org/0000-0001-9120-5578
Kuniaki Murase https://orcid.org/0000-0002-7564-9416

References

1. A. E. Rakhshani, *Solid State Electron.*, **29**, 7 (1986).
2. L. C. Olsen, F. W. Addis, and W. Miller, *Sol. Cells*, **7**, 247 (1982).
3. G. K. Paul, Y. Nawa, H. Sato, T. Sakurai, and K. Akimoto, *Appl. Phys. Lett.*, **88**, 141901 (2006).
4. Z. Q. Yu, C. M. Wang, M. H. Engelhard, P. Nachimuthu, D. E. McCready, I. V. Lyubinetsky, and S. Thevuthasan, *Nanotechnology*, **18**, 115601 (2007).
5. C. Zhu, A. Osherov, and M. J. Panzer, *Electrochim. Acta*, **111**, 771 (2013).
6. M. Izaki, T. Koyama, P. L. Khoo, and T. Shinagawa, *ACS Omega*, **5**, 683 (2020).
7. A. E. Rakhshani, A. A. Al-Jassar, and J. Varghese, *Thin Solid Films*, **148**, 191 (1987).
8. T. D. Golden et al., *Chem. Mater.*, **8**, 2499 (1996).
9. K. Mizuno, M. Izaki, K. Murase, T. Shinagawa, M. Chigane, M. Inaba, A. Tasaka, and Y. Awakura, *J. Electrochem. Soc.*, **152**, C179 (2005).
10. Y. Yang, D. Xu, Q. Wu, and P. Diao, *Sci. Rep.*, **6**, 35158 (2016).
11. K. Han and M. Tao, *Sol. Energy Mater. Sol. Cells*, **93**, 153 (2009).
12. J. Y. Ho and M. H. Huang, *J. Phys. Chem. C*, **113**, 14159 (2009).
13. M. Izaki, T. Shinagawa, K. Mizuno, Y. Ida, M. Inaba, and A. Tasaka, *J. Phys. D: Appl. Phys.*, **40**, 3326 (2007).
14. L. C. Wang, N. R. de Tacconi, C. R. Chenthamarakshan, K. Rajeshwar, and M. Tao, *Thin Solid Films*, **515**, 3090 (2007).
15. S. Joseph and P. V. Kamath, *J. Electrochem. Soc.*, **154**, E102 (2007).
16. T. Shinagawa, Y. Ida, K. Mizuno, S. Watase, M. Watanabe, M. Inaba, A. Tasaka, and M. Izaki, *Cryst. Growth Des.*, **13**, 52 (2013).
17. Y. Zhou and J. A. Switzer, *Scr. Mater.*, **38**, 1731 (1998).
18. T. Chen, A. Kitada, Y. Seki, K. Fukami, D. T. Usmanov, L. C. Chen, K. Hiraoka, and K. Murase, *J. Electrochem. Soc.*, **165**, D444 (2018).
19. T. Chen, A. Kitada, K. Fukami, and K. Murase, *J. Electrochem. Soc.*, **166**, D761 (2019).
20. M. Miyake, K. Murase, T. Hirato, and Y. Awakura, *J. Electrochem. Soc.*, **150**, C413 (2003).
21. K. S. Willson and J. A. Rogers, *Tech. Proc. American Electroplaters Society*, **51**, 92 (1964).
22. K. Inoue, T. Nakata, and T. Watanabe, *Mater. Trans.*, **43**, 1318 (2002).
23. N. G. Elfadill, M. R. Hashim, K. M. Chahrour, M. A. Qaeed, and M. Bououdina, *Superlattice. Microst.*, **85**, 908 (2015).
24. S. Bijani, L. Martínez, M. Gabás, E. A. Dalchiele, and J.-R. Ramos-Barrado, *J. Phys. Chem. C*, **113**, 19482 (2009).
25. H. Raebiger, S. Lany, and A. Zunger, *Phys. Rev. B*, **76**, 045209 (2007).
26. D. O. Scanlon, B. J. Morgan, G. W. Watson, and A. Walsh, *Phys. Rev. Lett.*, **103**, 096405 (2009).
27. J. Bahar, Y. Lghazi, B. Youbi, M. Ait Himi, C. El Haimer, A. Ouedrhiri, A. Aynaou, and I. Bimaghra, *Mater. Today Proc.*, **66**, 187 (2022).
28. J. S. Wilkes, J. A. Levisky, R. A. Wilson, and C. L. Hussey, *Inorg. Chem.*, **21**, 1263 (1982).
29. A. Kitada, K. Nakamura, K. Fukami, and K. Murase, *Electrochim. Acta*, **211**, 561 (2016).
30. K. Murase, M. Ogawa, T. Hirato, and Y. Awakura, *J. Electrochem. Soc.*, **151**, C798 (2004).
31. B. M. J. Siegfried and K.-S. Choi, *Adv. Mater.*, **16**, 1743 (2004).
32. M. M. Ferrer, G. S. L. Fabris, B. V. de Faria, J. B. L. Martins, M. L. Moreira, and J. R. Sambrano, *Heliyon*, **5**, e02500 (2019).
33. A. Soon, M. Todorova, B. Delley, and C. Stampfl, *Phys. Rev. B*, **75**, 125420 (2007).
34. Z. L. Wang, *J. Phys. Chem. B*, **104**, 1153 (2000).